Broadband ultrafast nonlinear optical response of few-layers graphene: toward the mid-infrared regime

Lili Miao,[1] Yaqin Jiang,[1] Shunbin Lu,[2] Bingxin Shi,[1] Chujun Zhao,[1,*] Han Zhang,[2] and Shuangchun Wen[1]

[1]*Key Laboratory for Micro-/Nano-Optoelectronic Devices of Ministry of Education, School of Physics and Electronics, Hunan University, Changsha 410082, China*

[2]*SZU-NUS Collaborative Innovation Center for Optoelectronic Science & Technology, Key Laboratory of Optoelectronic Devices and Systems of Ministry of Education and Guangdong Province, Shenzhen University, Shenzhen 518060, China*

**Corresponding author: chujunzhao@gmail.com*

Received April 10, 2015; revised July 8, 2015; accepted July 10, 2015; posted July 16, 2015 (Doc. ID 237862); published August 13, 2015

Gapless linear energy dispersion of graphene endows it with unique nonlinear optical properties, including broadband nonlinear absorption and giant nonlinear refractive index. Herein, we experimentally observed that few-layers graphene has obvious nonlinear absorption and large nonlinear refraction, as investigated by the Z-scan technique in the mid-infrared (mid-IR) regime. Our study may not only, for the first time to our knowledge, verify the giant nonlinear refractive index of graphene ($\sim 10^{-7}$ cm^2/W) at the mid-IR, which is 7 orders of magnitude larger than other conventional bulk materials, but also provide some new insights for graphene-based mid-IR photonics, potentially leading to the emergence of several new conceptual mid-IR optoelectronics devices.

OCIS codes: (160.4330) Nonlinear optical materials; (160.4760) Optical properties; (190.3270) Kerr effect.
http://dx.doi.org/10.1364/PRJ.3.000214

1. INTRODUCTION

Broadband nonlinear optical materials are needed urgently for numerous applications in different fields. Among the nonlinear optical materials, mid-infrared (mid-IR) nonlinear materials deserve more attention for their potential applications in spectroscopy, chemical, biomolecular sensing, security, and industry. It is not easy to find a material that exhibits excellent nonlinear performance and can be grown and fabricated with high optical quality.

Graphene, the first truly two-dimensional crystalline material, has been found to exhibit unique electronic and optical properties that have already aroused much scientific interest [1,2]. The remarkable optical property of graphene, featured by its ultra-broadband spectrum, stems from the linear dispersion energy band structure [3]. Its linear optical response is characterized by a universal conductivity, $\sigma_0 = e^2/4\hbar$, ranging from the visible to the mid-IR, suggesting that monolayer graphene exhibits a constant absorbance of about 2.3% [4]. With its efficient and relatively strong light–matter interaction, another fascinating property of graphene is its unique optical nonlinearities.

Despite its center-of-inversion symmetry, graphene also shows strong second-order nonlinear response that arises from symmetry breaking induced by the presence of a strong external electric field [5], the underlying substrate, the interfacial effects [6], and the presence of the radiation wave vector or its magnetic field [7]. The first nonzero high-order nonlinear optical term belongs to the third-order susceptibility that deserves our study in this contribution. The nonlinear optical properties of graphene at the visible, near-infrared, optical communication band, and even the microwave regime, include saturable absorption and nonlinear refraction. These properties and corresponding applications as a variety of photonic devices, such as passive mode lockers [8–14], ultrafast all-optical switches [15], optical power limiters [16], cascaded four-wave-mixing wavelength converters [17], and ultrafast all-optical modulators [18], have been experimentally demonstrated in the past few years [19–23]. Under intense light illumination, graphene's optical absorbance encounters a gradual decrease and becomes saturated at a certain level because of saturable absorption, which stems from the combined consequence of the Pauling blocking principle and the direct resonant absorption in graphene [24,25]. Strong light that propagates through a graphene layer might experience an additional nonlinear phase shift that may stem from the mass-less bandgap structure and the coherent electronic responses in graphene [26]. Owing to the linear dispersion band structure, which can cause resonances over a wide spectral range of photon energies, graphene was also theoretically predicted to possess a broadband nonlinear optical response. Moreover, the broadband third-order nonlinearity has been investigated by different approaches, the including four-wave mixing [27], spatial self-phase modulation [28], optical Kerr gate measurement [29], and Z-scan [26] methods. In spite of different experimental measurements on graphene's third-order nonlinearities, graphene shows large effective susceptibilities ($\chi^{(3)}_{\text{eff}}$) values.

The large $\chi^{(3)}$ has been verified experimentally in the near-infrared and the optical communication band. However, the mid-IR nonlinear optical properties related to $\chi^{(3)}$ and higher order nonlinearities of graphene have not yet been investigated. Moreover, the optical nonlinearity in graphene was theoretically predicated to be proportional to λ^4 [27], which implies that the nonlinear response will be better in the

mid-IR regime, which motivates a comprehensive investigation of the untouched mid-IR regime by using a high-quality graphene sample.

Enlightened by this fundamental interest, by employing a home-made mid-IR Z-scan measurement system where both open and closed aperture measurements could be performed, we are able to accurately identify the real and imaginary parts of the mid-IR third-order optical susceptibility of graphene for the first time, to the best of our knowledge. The measured results confirmed the excellent third-order nonlinear properties of graphene in the mid-IR regime.

2. HIGH-QUALITY GRAPHENE TRANSFER METHOD AND CHARACTERIZATION

Chemical vapor deposition (CVD)-grown graphene (ACS MATERIAL LLC, grown on Cu, 5 cm × 5 cm, six–eight layers) films were transferred to target substrates with the widely used polymethyl methacrylate (PMMA) transfer method. Different from other transfer methods, ultrasonic processing (UP) of target substrates was adopted to improve the transfer quality thanks to the improved hydrophilicity of the substrate [30].

The improved transfer quality was confirmed by the Raman characterization in Fig. 1. By analyzing the intensity ratio between the disorder-induced D band and the Raman-allowed G band, the higher I_D/I_G means more defects in the few-layers graphene (FLG) sample. Here, the I_D/I_G is about 0.2, indicating the graphene transferred onto the quartz has fewer defects [30].

The linear transmittance was also characterized for the FLG, as shown in Fig. 2. It can be seen that the graphene exhibits flat absorption ranging from 1000 to 2500 nm.

3. PUMP–PROBE EXPERIMENT

The ultrafast nonlinear response of FLG was investigated by time-resolved optical degenerate pump–probe measurement [31], with the experimental setup shown in Fig. 3. A femtosecond (fs) laser (Coherent Libra-S), which gave an output with a pulse repetition rate of 1 kHz, a central wavelength of 800 nm, and a pulse duration of around 100 fs, was employed in the time-resolved pump–probe experiment. The output was split into two different laser beams, one intense portion with a peak intensity of 75 GW/cm^2 as the pump beam to generate the photoinduced carriers, and the other weak portion with peak

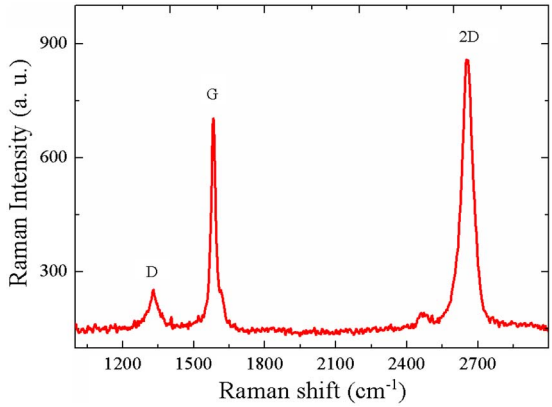

Fig. 1. Raman characterization of the graphene sample.

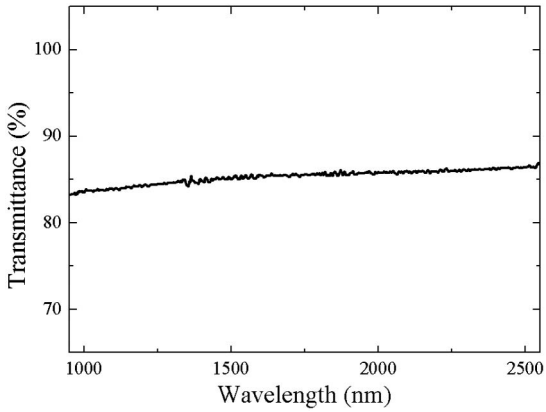

Fig. 2. Absorption spectra of six–eight-layer graphene.

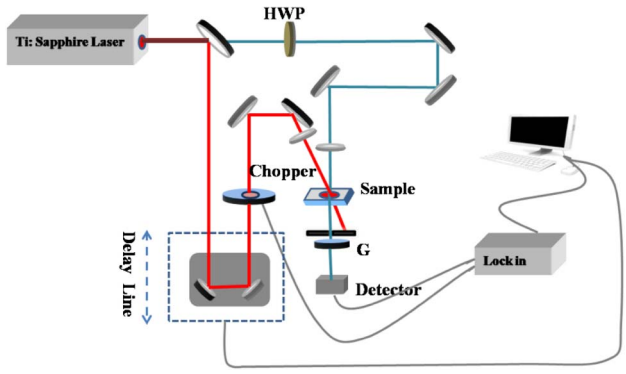

Fig. 3. Experimental setup of the pump–probe measurement.

intensity of 0.3 GW/cm^2 as the probe beam. The pump beam was focused onto the sample and spatially overlapped with the probe beam. The delay time between two pulses was controlled by a translation stage. The pump beam was modulated at a frequency of 290 Hz by a fast rotational chopper. The transmittance changes of the probe beam were recorded as a function of time delay between the pump and probe signal through a lock-in amplifier (SR850), providing internal detailed information about the carrier relaxation process occurring in the sample upon excitation. To minimize the scattering of the pump beam, we have to ensure that the probe and pump beams are orthogonally polarized through finely adjusting the half-wave plate (HWP) at the probe beam. By using a Glan–Taylor polarizer (G) with perpendicular polarization to the pump beam localized before the probe detector, we are able to sufficiently suppress the scattering of the pump beam.

The transient transmittance traces at different incident pump intensities measured on the FLG at room temperature are demonstrated in Fig. 4. The delay kinetics can be well fitted with a bi-exponential delay function:

$$\Delta T/T = A_1 e^{-t/\tau_1} + A_2 e^{-t/\tau_2}, \quad (1)$$

where $\Delta T/T$ is defined as the relative change of the probe transmissivity caused by the pump. τ_i is the decay time with the respective amplitude weights A_i. The fitting results show a similar fast time constant around 200 fs upon different pump intensity, which can be attributed to the ultrafast carrier

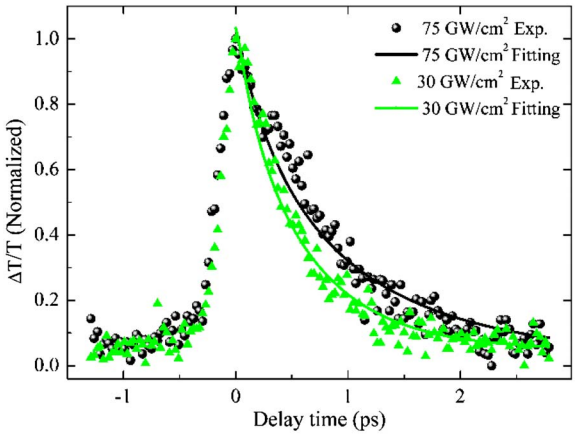

Fig. 4. Transient transmittance traces at different incident pump intensities for FLG at room temperature. The solid lines are fitting results based on different incident pump intensities.

thermalization in graphene via carrier–carrier scattering [32–34]. The slower time constants are around 1.07 and 2.0 ps under the pump intensities of 30 and 75 GW/cm^2, respectively. The pump intensity-dependent behavior was due to the carrier-photon scattering, which was well consistent with previously reported results [35]. Electron–hole recombination and cooling could also contribute to this slower decay time. At high excitation intensity, electron relaxation creates a large quantity of optical phonons, which could couple energy back into the electron distribution, and therefore slow down the cooling rate. Therefore, the value of the slow relaxation time at high pump intensity can determine the relaxation time for the optical phonon modes [36].

4. NONLINEAR OPTICAL RESPONSE OF FLG

We used 2 μm mode-locked ultrafast fiber laser source from AdValue Photonics with center wavelength of 1930 nm, pulse repetition rate of 32.3 MHz, and pulse duration of 2.8 ps to implement the nonlinear measurements.

Based on a self-made Z-scan system, the nonlinear measurements were implemented in both open-aperture (OA) and closed-aperture (CA) regimes, wherein all/part of the light transmitted through the sample was collected on a photodetector, as shown in Fig. 5. The OA regime enables characterization of the intensity-dependent absorption, and the closed one corresponds to the nonlinear refractive index properties. By analyzing OA and CA measurements, the saturable absorption properties and n_2 were obtained. The laser beam was focused by using a CaF_2 lens with a focal length of 150 mm. The average focused spot size was about 35 μm,

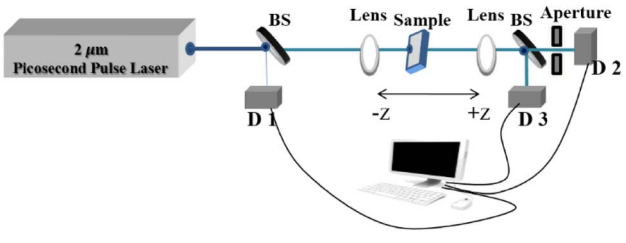

Fig. 5. Experimental setup of the Z-scan measurement.

further confirmed by Z-scan parameter fitting, corresponding to a peak intensity of 57.5 MW/cm^2. In the experiment, the far-field condition for the aperture plane ($d \gg z_0$) was satisfied, where d is the propagation distance in free space from the sample to the aperture plane, and z_0 is the diffraction length of the beam. During the measurement, we adjusted the radius of the aperture to make the linear transmittance S of the aperture equal to 0.1, where $S = 1 - \exp(-2r_a/w_a)$, r_a is the aperture radius, and w_a is the laser beam radius on the aperture.

The graphene samples and its quartz substrate were oriented perpendicularly to the beam axis and translated along the axis through the focus with a motorized precision translation stage.

The transmitted power was recorded by the detector (Newport 818P-001-12) placed in the far field of the focal beam spot with either no aperture or a small aperture. The incident beam intensity was detected by a reference detector. A computer-controlled powermeter was used to measure the optical power. To make the experimental results valid, the same sample was moved from +Z to –Z, and then –Z to +Z. In addition, we spatially changed the graphene sample illumination area, and repeatable results could be obtained. In our experiment, no external field is introduced, and phase-matching alignments have not been paid attention. During the experiments, the average focused spot size was about 35 μm, and the measurement result reports the averaged size, which means that layer changes in the illumination area cannot be distinguished. The high-quality graphene samples combined with microzone analysis will be introduced in further measurements. Moreover, second-harmonic generation could not be observed by adjusting the power or moving the lens. We argue that the second-order nonlinearity will not be involved in the measurements.

According to Fig. 6, it is obvious that the optical nonlinear effect of the substrate was negligible comparing to graphene. The ratio of the linear transmitted power between the graphene sample and the substrate is about 14.9%, which is close to the theoretical transmittance of FLG, indicating that this graphene sample is the six–eight layer graphene. The nonlinear effect of graphene is closely relevant to the photon excited time, thus the interplay between intraband and interband dynamics should be considered to describe the nonlinear

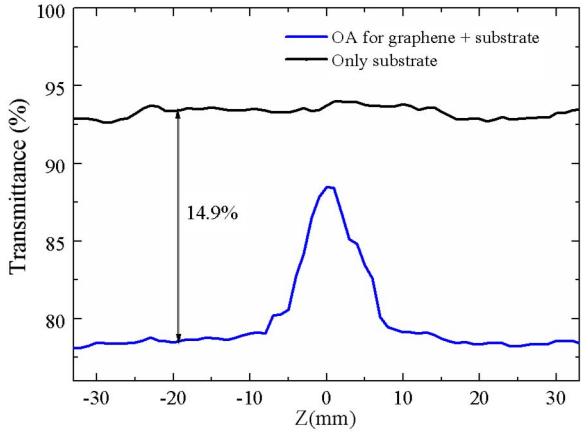

Fig. 6. Curves of an OA Z-scan by FLG sample. The black curve represents the quartz substrate, and the blue curve represents the FLG sample on quartz.

optical response in graphene. Photoexcited electron–hole pairs thermalize via carrier–carrier intraband scattering and phonon emission on a femtosecond time scale to reach a new Fermi–Dirac distribution. This is followed by interband carrier relaxation and hot phonon emission on the picosecond time scale [25], which is consistent with our pump–probe results of the FLG carrier dynamics, where fast and slower time constants are around 200 fs and 1.07–2.0 ps, respectively.

For the OA data, the saturable absorption process leads to the strong transmission rise at the focus $z = 0$ at 1930 nm. Figure 7(a) shows the typical curves of Z-scan measurements for 1930 nm. The nonlinear optical response (SA) of FLG at 1930 nm was further confirmed by the balanced twin detector method, as shown in Fig. 7(b).

Typical CA measurements are shown in Figs. 8(a)–8(d). The apparent peak and valley in the CA data shows contributions from both nonlinear refraction and saturable absorption. The up–down curve implies a small positive on-axis phase shift $\Delta\Phi$.

For graphene, a simple two-level saturable absorption can be modeled by the following equation:

$$\alpha^*(N) = \frac{\alpha_S^*}{1 + \frac{I}{I_s}} + \alpha_{NS}^*, \tag{2}$$

where I_s characterizes the saturation intensity, defined as the optical intensity required in a steady state to reduce the absorption to half of its unbleached value. The incident intensity I is concerned with the location of the sample. α_s^* and α_{NS}^* represent the saturable and nonsaturable losses, respectively.

Herein, to analyze the Z-scan data of graphene saturable absorption, we use the normalized transmittance formula based on one photon absorption:

$$T = \left(1 - \frac{\alpha_0 L}{1 + I/I_s}\right) \cdot \frac{1}{1 - \alpha_0 L}, \tag{3}$$

where α_0 characterizes the linear absorption index and L represents the sample length.

For the CA results, one can fit the curve with the following function:

$$T(x) = 1 + \frac{4x\Delta\Phi}{(1 + x^2)(9 + x^2)}, \tag{4}$$

where $x = z/z_0$ is the normalized distance from the focus and z_0 is the Rayleigh length. The above method for deriving $\Delta\Phi$ from the measured data is applicable when the distortion of the phase front is small and the closed aperture is sufficiently narrow [37]. The nonlinear refractive index can be obtained using $n_2 = \Delta\Phi/(k_0 L_{\text{eff}} I)$, where $k_0 = 2\pi/\lambda$ and L_{eff} is the effective thickness of the FLG sample.

It can be seen in Fig. 7(a) that the modulation depth and saturation intensity are about 12% and 1 MW/cm^2, respectively. We also measured the same sample at 1562 nm (20.8 MHz, 1.5 ps), as shown in Fig. 8(b), and the modulation depth and saturation intensity are 8% and 117 MW/cm^2, which is of the same order of magnitude as the value reported in [26]. A values of n_2 of 4.58×10^{-7} and 1.64×10^{-7} cm^2/W were obtained at 1930 and 1562 nm, respectively, which is of the same order of magnitude as the value reported in [38], approximately 10^7 times larger than that of bulk dielectrics. The ratio of n_2 at 1.93 and 1.56 μm is about 2.8, which has deviation from the scale law by λ^4, i.e., 2.3. The deviation can be attributed to the experimental errors, such as the determination of beam waist, the slow response of the power detectors, and so on. Semnani *et al.* calculated the third-order susceptibility and nonlinear refractive index theoretically; the theoretical prediction for the Kerr coefficient $n_2 \approx 10^{-7}$ cm^2/W, and it is weakly frequency dependent in a wide range of frequencies (from the visible to infrared) [38]. The chirality leads to a remarkably strong nonlinear optical response, which was classified as pure intraband, pure interband, or a combination of the both. However, the Z-scan measurements reported here measure the sum of all contributions to n_2, such as nonparametric processes that gives rise to both saturable absorption and n_2. Of course, the different measuring methods (Z-scan to four-wave mixing) and conditions (i.e., pulse width) may contribute to the difference.

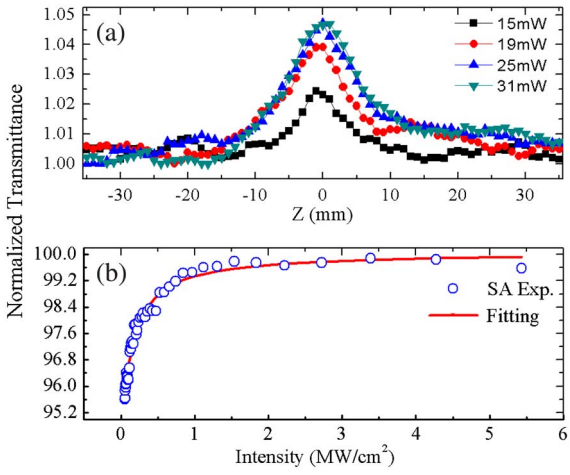

Fig. 7. (a) Power-dependent transmittance of FLG, and (b) balanced twin detector of FLG.

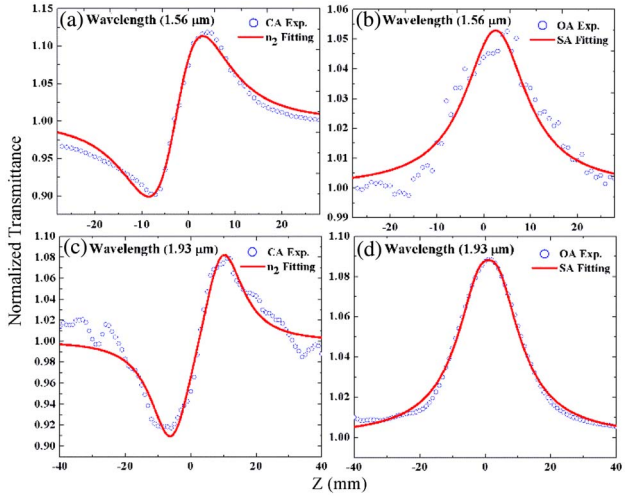

Fig. 8. (a) CA Z-scan measurement of FLG at 1.56 μm, (b) OA Z-scan measurement of FLG at 1.56 μm, (c) CA Z-scan measurement of FLG at 1.93 μm, and (d) OA Z-scan measurement of FLG at 1.93 μm.

5. DISCUSSION

The development of mid-IR photonics has been limited by the lack of suitable mid-IR optical materials. The unique mid-IR saturable absorption and significant Kerr nonlinearity in graphene could promote the development of mid-IR photonics in two different aspects. One concerns the ultrashort pulse generation based on its saturable absorption and the other is correlated with the mutual nonlinear interaction of mid-IR laser beams based on Kerr nonlinearity. Ultrashort pulse lasers are already regarded as important tools for various applications in medical imaging, high-speed optical communication, and industrial processing [39,40]. Among all the ultrafast pulse generation approaches, passive mode-locking is considered the most direct approach to yield ultrashort pulses. However, to initial and sustain passive mode-locking operation, one has to incorporate an intensity discriminating component inside the laser cavity, such as an optical saturable absorber device. However, producing a low-cost and practical saturable absorber that could stably operate around 2 μm remains a challenge because of complicated fabrication methods and large intrinsic loss, which might limit the advancement of mid-IR ultrashort pulse lasers. The broadband saturable absorption property of graphene might clear the obstacles and therefore foster the development of mid-IR photonics. Second, manipulating a mid-IR laser beam by the nonlinear Kerr effect remains troublesome because of the lack of suitable nonlinear Kerr materials with strong nonlinear Kerr refractive index but relatively low optical loss. Recently, stable mode-locking of bulk lasers at wavelengths near 1, 2, and 2.4 μm has been demonstrated by the contribution of Kerr lens effect and saturable absorption effect of gold-film graphene at the mid-IR [14].

Based on the experimental results, it is argued that graphene is a promising nonlinear optical material that may be fit for high-power mid-IR operation. Despite its atomic thickness, it can still induce significant phase shift under high-power excitation because of its remarkable nonlinear Kerr refractive index. Moreover, its absorbance will decrease with the increase of pump power and it will become almost transparent once the pump power exceeds a threshold, making its figure of merit (FOM), the ratio of nonlinear phase shift with respect to the absorbance [41], very attractive at the high-power regime. We use the definition of FOM for third-order nonlinearity as $\mathrm{FOM} = |\Delta n/(\alpha\lambda)|$, where Δn is the refractive index change at the focal point, and α is the absorption coefficient [42]. The FOM was calculated to be 1.02 and 1.6 for the 1930 and 1562 nm lasers, respectively. In association with its advantages of excellent mechanical properties and high thermal conductivity, graphene is therefore suggested to be highly favorable (high nonlinear phase and low absorption per layer) for integrated mid-IR photonics. Given that chemical potential plays an important role in the origin of optical nonlinearity, we are able to deliberately tailor its nonlinear optical response by electrical tuning or chemical doping. For example, by tuning the Fermi energy level, its linear absorbance could be significantly suppressed while its nonlinear phase shift remained remarkable, allowing for generation of desired nonlinearities with higher FOM. This type of band engineering will definitely help researchers fabricate novel graphene-based nonlinear optical devices.

6. CONCLUSIONS

We have experimentally measured the third-order nonlinear response of CVD-grown FLG based on a mid-IR Z-scan setup. Particularly, the real and imaginary parts of its third-order susceptibility, including the saturable absorption and nonlinear refraction around 2 μm, have been identified for the first time, to the best of our knowledge. Its mid-IR saturable absorption property makes it able to be developed as an effective saturable absorber for ultrashort mid-IR pulse generation. Its significant mid-IR Kerr nonlinearity might stimulate a new wave of exploration into graphene-based Kerr photonics. More fundamentally, our demonstration opens an avenue for the feasibility of manipulating light toward the mid-IR regime, by taking into account the confirmed Kerr nonlinearity in graphene, empowered by the ultrafast response time, high damage threshold, and low intrinsic loss. It might eventually enable new mid-IR nonlinear optical devices based on graphene and other two-dimensional materials.

ACKNOWLEDGMENT

This work is partially supported by the National 973 Program of China (Grant No. 2012CB315701), and the National Natural Science Foundation of China (Grant Nos. 61205125, 61222505, and 61475102).

REFERENCES

1. A. K. Geim, "Graphene: status and prospects," Science **324**, 1530–1534 (2009).
2. A. H. Castro Neto, F. Guinea, N. M. R. Peres, K. S. Novoselov, and A. K. Geim, "The electronic properties of graphene," Rev. Mod. Phys. **81**, 109–162 (2009).
3. F. Bonaccorso, Z. Sun, T. Hasan, and A. C. Ferrari, "Graphene photonics and optoelectronics," Nat. Photonics **4**, 611–622 (2010).
4. R. R. Nair, P. Blake, A. N. Grigorenko, K. S. Novoselov, T. J. Booth, T. Stauber, N. M. R. Peres, and A. K. Geim, "Fine structure constant defines visual transparency of graphene," Science **320**, 1308 (2008).
5. S. Wu, L. Mao, A. M. Jones, W. Yao, C. Zhang, and X. Xu, "Quantum-enhanced tunable second-order optical nonlinearity in bilayer graphene," Nano Lett. **12**, 2032–2036 (2012).
6. J. J. Dean and H. M. van Driel, "Second harmonic generation from graphene and graphitic films," Appl. Phys. Lett. **95**, 261910 (2009).
7. M. Glazov, "Second harmonic generation in graphene," JETP Lett. **93**, 366–371 (2011).
8. Z. Sun, T. Hasan, F. Torrisi, D. Popa, G. Privitera, F. Wang, F. Bonaccorso, D. M. Basko, and A. C. Ferrari, "Graphene mode-locked ultrafast laser," ACS Nano **4**, 803–810 (2010).
9. L. M. Zhao, D. Y. Tang, H. Zhang, X. Wu, Q. Bao, and K. P. Loh, "Dissipative soliton operation of an ytterbium-doped fiber laser mode locked with atomic multilayer graphene," Opt. Lett. **35**, 3622–3624 (2010).
10. H. Zhang, D. Tang, R. J. Knize, L. Zhao, Q. Bao, and K. P. Loh, "Graphene mode locked, wavelength-tunable, dissipative soliton fiber laser," Appl. Phys. Lett. **96**, 111112 (2010).
11. G. Sobon, "Mode-locking of fiber lasers using novel two-dimensional nanomaterials: graphene and topological insulators [Invited]," Photon. Res. **3**, A56–A63 (2015).
12. J. Ma, G. Xie, P. Lv, W. Gao, P. Yuan, L. Qian, H. Yu, H. Zhang, J. Wang, and D. Tang, "Graphene mode-locked femtosecond laser at 2 μm wavelength," Opt. Lett. **37**, 2085–2087 (2012).
13. W. Tan, C. Su, R. Knize, G. Xie, L. Li, and D. Tang, "Mode locking of ceramic Nd:yttrium aluminum garnet with graphene as a saturable absorber," Appl. Phys. Lett. **96**, 031106 (2010).
14. J. Ma, G. Xie, P. Lv, W. Gao, P. Yuan, L. Qian, U. Griebner, V. Petrov, H. Yu, and H. Zhang, "Wavelength-versatile graphene-gold film saturable absorber mirror for ultra-broadband mode-locking of bulk lasers," Sci. Rep. **4**, 5016 (2014).

15. M. Oya, H. Kishikawa, N. Goto, and S.-I. Yanagiya, "All-optical switch consisting of two-stage interferometers controlled by using saturable absorption of monolayer graphene," Opt. Express **20**, 27322–27330 (2012).
16. P. Chantharasupawong, R. Philip, N. T. Narayanan, P. M. Sudeep, A. Mathkar, P. M. Ajayan, and J. Thomas, "Optical power limiting in fluorinated graphene oxide: an insight into the nonlinear optical properties," J. Phys. Chem. C **116**, 25955–25961 (2012).
17. Y. Wu, B. Yao, Q. Feng, X. Cao, X. Zhou, Y. Rao, Y. Gong, W. Zhang, Z. Wang, and Y. Chen, "Generation of cascaded four-wave-mixing with graphene-coated microfiber," Photon. Res. **3**, A64–A68 (2015).
18. W. Li, B. Chen, C. Meng, W. Fang, Y. Xiao, X. Li, Z. Hu, Y. Xu, L. Tong, and H. Wang, "Ultrafast all-optical graphene modulator," Nano Lett. **14**, 955–959 (2014).
19. J. Wang, Y. Hernandez, M. Lotya, J. N. Coleman, and W. J. Blau, "Broadband nonlinear optical response of graphene dispersions," Adv. Mater. **21**, 2430–2435 (2009).
20. Z. Zheng, C. Zhao, S. Lu, Y. Chen, Y. Li, H. Zhang, and S. Wen, "Microwave and optical saturable absorption in graphene," Opt. Express **20**, 23201–23214 (2012).
21. H. Yang, X. Feng, Q. Wang, H. Huang, W. Chen, A. T. Wee, and W. Ji, "Giant two-photon absorption in bilayer graphene," Nano Lett. **11**, 2622–2627 (2011).
22. J. Zhou, A. Luo, Z. Luo, X. Wang, X. Feng, and B.-O. Guan, "Dual-wavelength single-longitudinal-mode fiber laser with switchable wavelength spacing based on a graphene saturable absorber," Photon. Res. **3**, A21–A24 (2015).
23. Z. Liu, X. Zhang, X. Yan, Y. Chen, and J. Tian, "Nonlinear optical properties of graphene-based materials," Chin. Sci. Bull. **57**, 2971–2982 (2012).
24. R. N. Zitter, "Saturated optical absorption through band filling in semiconductors," Appl. Phys. Lett. **14**, 73–74 (1969).
25. Q. Bao, H. Zhang, Y. Wang, Z. Ni, Y. Yan, Z. X. Shen, K. P. Loh, and D. Y. Tang, "Atomic-layer graphene as a saturable absorber for ultrafast pulsed lasers," Adv. Funct. Mater. **19**, 3077–3083 (2009).
26. H. Zhang, S. Virally, Q. Bao, L. K. Ping, S. Massar, N. Godbout, and P. Kockaert, "Z-scan measurement of the nonlinear refractive index of graphene," Opt. Lett. **37**, 1856–1858 (2012).
27. E. Hendry, P. J. Hale, J. Moger, A. K. Savchenko, and S. A. Mikhailov, "Coherent nonlinear optical response of graphene," Phys. Rev. Lett. **105**, 097401 (2010).
28. R. Wu, Y. Zhang, S. Yan, F. Bian, W. Wang, X. Bai, X. Lu, J. Zhao, and E. Wang, "Purely coherent nonlinear optical response in solution dispersions of graphene sheets," Nano Lett. **11**, 5159–5164 (2011).
29. S. Chu, S. Wang, and Q. Gong, "Ultrafast third-order nonlinear optical properties of graphene in aqueous solution and polyvinyl alcohol film," Chem. Phys. Lett. **523**, 104–106 (2012).
30. G. Zheng, Y. Chen, H. Huang, C. Zhao, S. Lu, S. Chen, H. Zhang, and S. Wen, "Improved transfer quality of CVD-grown graphene by ultrasonic processing of target substrates: applications for ultra-fast laser photonics," ACS Appl. Mater. Interfaces **5**, 10288–10293 (2013).
31. C. Gao, X. Zhao, J. Yao, X.-Q. Yan, X. T. Kong, Y. Chen, Z. B. Liu, and J. G. Tian, "Sign of differential reflection and transmission in pump-probe spectroscopy of graphene on dielectric substrate," Photon. Res. **3**, A1–A9 (2015).
32. J. M. Dawlaty, S. Shivaraman, M. Chandrashekhar, F. Rana, and M. G. Spencer, "Measurement of ultrafast carrier dynamics in epitaxial graphene," Appl. Phys. Lett. **92**, 042116 (2008).
33. M. Breusing, S. Kuehn, T. Winzer, E. Malić, F. Milde, N. Severin, J. Rabe, C. Ropers, A. Knorr, and T. Elsaesser, "Ultrafast nonequilibrium carrier dynamics in a single graphene layer," Phys. Rev. B **83**, 153410 (2011).
34. E. Malic, T. Winzer, E. Bobkin, and A. Knorr, "Microscopic theory of absorption and ultrafast many-particle kinetics in graphene," Phys. Rev. B **84**, 205406 (2011).
35. F. Rana, "Electron-hole generation and recombination rates for Coulomb scattering in graphene," Phys. Rev. B **76**, 155431 (2007).
36. L. Huang, G. V. Hartland, L.-Q. Chu, R. M. Feenstra, C. Lian, K. Tahy, and H. Xing, "Ultrafast transient absorption microscopy studies of carrier dynamics in epitaxial graphene," Nano Lett. **10**, 1308–1313 (2010).
37. M. Sheik-Bahae, A. A. Said, T.-H. Wei, D. J. Hagan, and E. W. Van Stryland, "Sensitive measurement of optical nonlinearities using a single beam," IEEE J. Quantum Electron. **26**, 760–769 (1990).
38. B. Semnani, A. H. Majedi, and S. Safavi-Naeini, "Nonlinear quantum optical properties of graphene: the role of chirality and symmetry," arXiv:1502.02203 (2015).
39. G. Sucha, "Overview of industrial and medical applications of ultrafast lasers," in *Handbook of Ultrafast Lasers: Technology and Applications*, M. E. Fermann, A. Galvanauskas, and G. Sucha, eds. (Academic, 2003), pp. 286–316.
40. J. A. Salehi, A. M. Weiner, and J. P. Heritage, "Coherent ultrashort light pulse code-division multiple access communication systems," J. Lightwave Technol. **8**, 478–491 (1990).
41. G. Lenz, J. Zimmermann, T. Katsufuji, M. Lines, H. Hwang, S. Spälter, R. Slusher, S.-W. Cheong, J. Sanghera, and I. Aggarwal, "Large Kerr effect in bulk Se-based chalcogenide glasses," Opt. Lett. **25**, 254–256 (2000).
42. Y. Lin, J. Zhang, E. Kumacheva, and E. Sargent, "Third-order optical nonlinearity and figure of merit of CdS nanocrystals chemically stabilized in spin-processable polymeric films," J. Mater. Sci. **39**, 993–996 (2004).